DOI: 10.3969/j.issn.1673-3185.2016.06.005 **http:** // english.ship-research.com

Translated from: YI Xiuyang, ZHOU Qidou, WU Xiangxing. Simulating calculation and experimental investigation on acoustic transmitting characteristics of the testing field in limited waters[J]. Chinese Journal of Ship Research, 2016, 11(6): 28-34, 39.

Simulating calculation and experimental investigation on acoustic propagation characteristics of the testing field in limited water area

YI Xiuyang[1], *ZHOU Qidou*[1], *WU Xiangxing*[2]

1 Department of Naval Architecture Engineering, Naval University of Engineering, Wuhan 430033, China
2 Hangzhou Applied Acoustic Research Institute, Hangzhou 310023, China

Abstract: When vibration and noise control experiments of large complicated structures are conducted in limited water areas, the core aspects are acoustic signal measurement and data processing. The boundary conditions are complex and unknown, and the hydrological environment and acoustic propagation characteristics are intricate, which causes greater difficulties for the numerical simulation and data processing of the signal. AcTUP, a combined program developed by Matlab and VB codes, is adopted to analyze the selection principles of the water level and the sedimentary layers of the testing field, obtaining a simulation model that coincides with experimental values. In this paper, via simulating calculation and analysis, the influence discipline of 'zero dimension' parameters concerning fixed depth source, source position of constant water depth and water surface roughness on acoustic transmission loss are obtained, then certain basic acoustic propagation characteristics of the field are acquired through an incoherent analysis of the deviations between experimental values and simulating values based on ray theory.

Key words: limited water area; acoustic testing field; acoustic propagation characteristics; boundary conditions; AcTUP; ray theory; deviation

CLC number: U666.7

0 Introduction

Submarine has become one of the national strategic deterrent arms because of its stealth. The acoustic stealth performance of submarine has been obviously enhanced by the technologies of anechoic tile, floating raft isolation, acoustic stealth material, etc. Known as the "black hole of the oceans", the radiative sound source level of "Kilo" conventional submarine corresponds to that of marine environment, which has raised the wave of acoustic stealth technology revolution. The simulation of acoustic vibration characteristics of cylindrical shells is usually used in the study of acoustic characteristics of submarine[1-2], but the reliability of the simulation must be verified by experiments. The testing field in limited water area has a relatively wide space, which is the first choice for underwater acoustic stealth performance of large structures. In order to reduce the influence of boundary conditions on the measurement accuracy of test, the Department of Underwater Acoustics of U S Navy Institute used high-pressure anechoic pool to study the acoustic characteristics of submarine, but the construction technology, performance of acoustic material and construction cost limited its application object. Therefore, the selection of natural testing

Received: 2016-05-06

Supported by: National Ministries Foundation

Author(s): YI Xiuyang, male, born in 1990, master candidate. Research interest: acoustics stealth technique of ship. E-mail: oucyxy@163.com

ZHOU Qidou (Corresponding author), male, born in 1962, professor, doctoral supervisor. Research interest: hydrodynamic force and structural vibration noise control. E-mail: qidou_zhou@126.com

field in limited water area has garnered scholars' favor.

The study on the acoustic propagation characteristics in natural limited water area including rivers, lakes and seas, has become the precondition of underwater acoustic warfare of submarine. Jensen et al.[3] pointed out that acoustic propagation had the best frequency, which was closely related to the water depth, the acoustic velocity profile and the underwater type. Internationally, the development of computational ocean acoustics[4], as well as the progress of acoustic modeling and simulation technology[5], not only broadened our thinking in this paper, but also laid a theoretical foundation for simulating calculation. Chen[6] studied the acoustic characteristics of the paralic environment based on codes of Kraken, Bellhop, and Ray for 3D, and pointed out that the ocean's acoustic propagation characteristics can be described by the acoustic ray stability parameter; Lin et al.[7] studied the acoustic propagation characteristics of mesoscale marine environment using ray stability parameters and wave invariants, which provided a feasible basis for the numerical simulation of this paper; Chen et al.[8] explored the effects of hydrological conditions on active acoustic detection system signal using ray theory and Bellhop model, which provided references for the selection of limited water area simulation model in this study; Chen[9] proposed a prediction method of acoustic radiation characteristics of underwater elastomer based on theory and experiment, providing a guidance of systematic methodology for this paper.

In the above references, the acoustic propagation characteristics in ocean or unlimited water area and the acoustic vibration characteristics of structures immersed in them were researched, but research on the acoustic propagation characteristics of acoustic testing field in limited water area was still in its infancy. In this paper, combined with the acoustic theory, simulating calculation on acoustic characteristics of testing field will be carried out using AcTUP, a combined programming software developed by Matlab and VB[10], ideas of modeling parameters setting will be provided, and acoustic propagation characteristics of acoustic testing field in limited water area will be obtained, which provides technical support for engineering application.

1 Acoustic theory and computational methods

The wave equation of acoustic testing field in limited water area is

$$\nabla^2 P - \frac{1}{c^2}\frac{\partial^2 P}{\partial t^2} = -S(t)\frac{\delta(z-z_s)\delta(r)}{2\pi r} \tag{1}$$

where P is acoustic pressure, Pa; c is acoustic velocity, m/s; r is distance from field point to sound source, m; $S(t)$ is the sound source's spectrum information; δ is to describe the singularity condition; z is the water depth, m; and z_s is the source depth, m.

There are 2 methods for solving the wave equation: normal mode theory and ray acoustics. Their corresponding program computational model are normal mode (Kraken) and ray (Bellhop), but the Kraken algorithm is only suitable for remote low frequency, and Bellhop algorithm is only suitable for short-range high frequency. Therefore, a single calculation model cannot satisfy the study of the acoustic propagation characteristics of acoustic testing field. The ScooterFields fast field model[11] is used in this paper, whose essence is to express the solution of the wave equation in the form of wave number integral, and to realize high precision and fast rate of calculation of integral through the Fourier transform method, including both discrete mode and continuous mode.

Because of its intuition, ray acoustics is usually adopted to describe the acoustic energy and acoustic propagation path. The acoustic properties of experimental field are studied by using resonance wave $p=\frac{1}{R}e^{-jkR}$ with a spectrum signal of sound source of 1. It is assumed that the water surface and bottom are absolutely soft and rigid boundaries, reflected acoustic rays of surface and bottom are considered acoustic rays sent by symmetrical "image point" of boundary, and the total acoustic field is the result of superposition of sound source and the infinite "image points", as shown in Fig. 1. In the figure, O_{01} is sound source; O_{02}-O_{04} are the virtual source of bound-

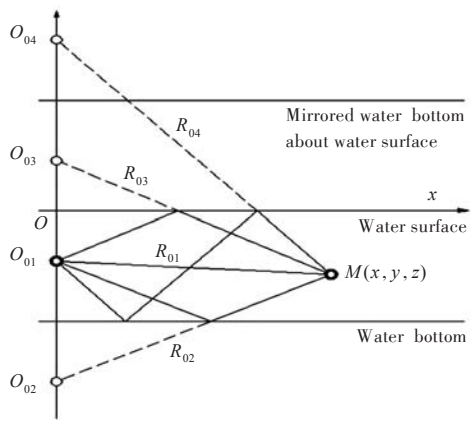

Fig.1 Virtual sources and reflected waves

ary reflection; M is any acoustic field point; and R is distance between field point and image point.

The boundary loss coefficient and medium absorption coefficient are neglected, and the expression of acoustic pressure that meets the boundary conditions of water surface and bottom is

$$P=\sum_{m=0}^{\infty}(-1)^m \left[\frac{1}{R_{m1}}\mathrm{e}^{\mathrm{j}kR_{m1}}+\frac{1}{R_{m2}}\mathrm{e}^{\mathrm{j}kR_{m2}}-\frac{1}{R_{m3}}\mathrm{e}^{\mathrm{j}kR_{m3}}-\frac{1}{R_{m4}}\mathrm{e}^{\mathrm{j}kR_{m4}}\right] \quad (2)$$

In the formula, $R_{mi}=\sqrt{x^2+y^2+z_{mi}^{\ 2}}$ is the distance between field point and image point, where $m=0,1,2,\cdots,\infty$, $i=1,2,3,4$.

$$\begin{cases} z_{m1}=2\times 70\times m-z+12.5 \\ z_{m2}=2\times 70\times (m+1)-z-12.5 \\ z_{m3}=2\times 70\times m+z+12.5 \\ z_{m4}=2\times 70\times (m+1)-z-12.5 \end{cases} \quad (3)$$

Eq. (2) is from the section of ray acoustics in the principles of underwater sound[12-13], and Eq. (3) is modified in this paper according to the testing field boundary.

2 Experimental study

Through the hydrological survey, the testing field can be regarded as cylindrical symmetry. The depth of water is 70 m, and the single-frequency shock excitation sound source is located at 12.5 m below the water surface. Fig. 2 and Fig. 3 are the general arrangement and the scene drawing of the acoustic experiment. In order to study the acoustic propagation characteristics of the testing field in 60-1 000 Hz, the sound pressure level at about 35 and 255 m from the sound source is measured by the standard sound source, and the transmission loss TL at the acoustic field point is calculated according to Eq. (4)

$$TL=PL_{\text{experiment}}-SPL \quad (4)$$

where $PL_{\text{experiment}}$ is measured sound pressure level, and SPL is standard sound pressure level.

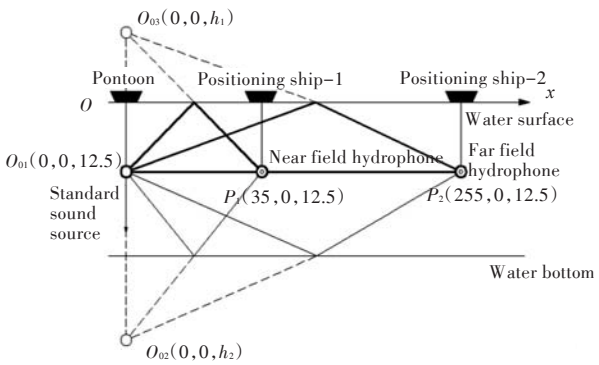

Fig.2 Arrangement of testing field

Fig.3 Testing field in limited water

2.1 Test instruments

Standard sound source selected in the experiment is constituted by a piezoelectric ceramic transducer and a standard hydrophone at unit distance right above it. It has no directivity, the sensitivity of -190 dB, the SNR no less than 30 dB, and can realize the low frequency transduction. MODEL L6 power amplifier is at kilowatt level (Fig. 4).

Fig.4 Standard sound source and power amplifier

2.2 Test methods

The steps of the test are:

1) The standard sound source is placed at 12.5 m below the water surface to simulate the position of the structural underwater force excitation.

2) According to the differential GPS positioning system, hydrophones of the same depth are set at 35 and 255 m from the standard sound source, respectively.

3) The parameters of MODEL L6 are adjusted, and the electrical signals of different frequencies and transmitting voltages are changed into acoustic signals of the transducer, then the underwater shock excitation signal of transducer can be transmitted to the power amplifier by standard hydrophone, which is converted into visual electrical signals. The transmitting voltage response S_{V} of transducer and the radiative sound pressure level SL of sound source when calibrated in the testing field can be obtained by Eq. (5)-(6).

$$S_V = 20\lg\left[\frac{U_J \times d}{U_F}\right] - M_0 - 60 \quad (5)$$

$$SL = 20\lg\left[\frac{U_J \times d}{2\,830}\right] - M_0 \quad (6)$$

where U_J is the receiving voltage of MODEL L6 when sound source is calibrated in the testing field, mV; U_F is transmitting voltage of MODEL L6 when sound source is calibrated in the testing field, mV; and d is the vertical distance between the standard hydrophone and the transducer.

4) Signal parameters of MODEL L6 are readjusted, and near field sound pressure level P_{near} and far field sound pressure level P_{far} of single frequency 60–1 000 Hz are measured. The standard sound source pressure level *SPL* is obtained according to Eq. (7).

$$SPL = 20\lg\left[\frac{U_{JS} \times d}{2\,830}\right] - M_0 \quad (7)$$

where U_{JS} is experimental receiving voltage.

5) According to Eq.(8), the measured transmission loss is obtained, and the comparison between the experimental value and the simulation value is realized.

$$TL = SPL - PL_{measurement} \quad (8)$$

3 Simulating calculation of acoustic characteristics of testing field

3.1 Acoustic simulation model

3.1.1 Selection of "sedimentary layers" model

The acoustic propagation characteristics of acoustic testing field in limited water area are closely related to the boundary conditions, and the key is to find the most practical underwater boundary. According to the preliminary survey of testing field construction and probe reconnaissance, underwater sedimentary layers with 2 kinds of acoustic characteristics are obtained, as shown in Table 1. In the table: ρ is density; c is acoustic velocity; and α_ω is the attenuation coefficient of unit wavelength.

Table 1 Acoustic characteristics of underwater sedimentary layers

	ρ/(kg·m^{-3})	c/(m·s^{-1})	α_ω/dB
"Mud–sand" type	1 787	1 652	1.17
"Slime–clay" type	1 491	1 549	0.148

Through the simulating calculation, acoustic transmission loss of the near field and the far field sedimentary layers of "mud–sand" and "slime–clay" types is obtained, which is acoustically contrasted with the test values and the theoretical loss values of the cylindrical, transitional and spherical wave expansions (Fig. 5).

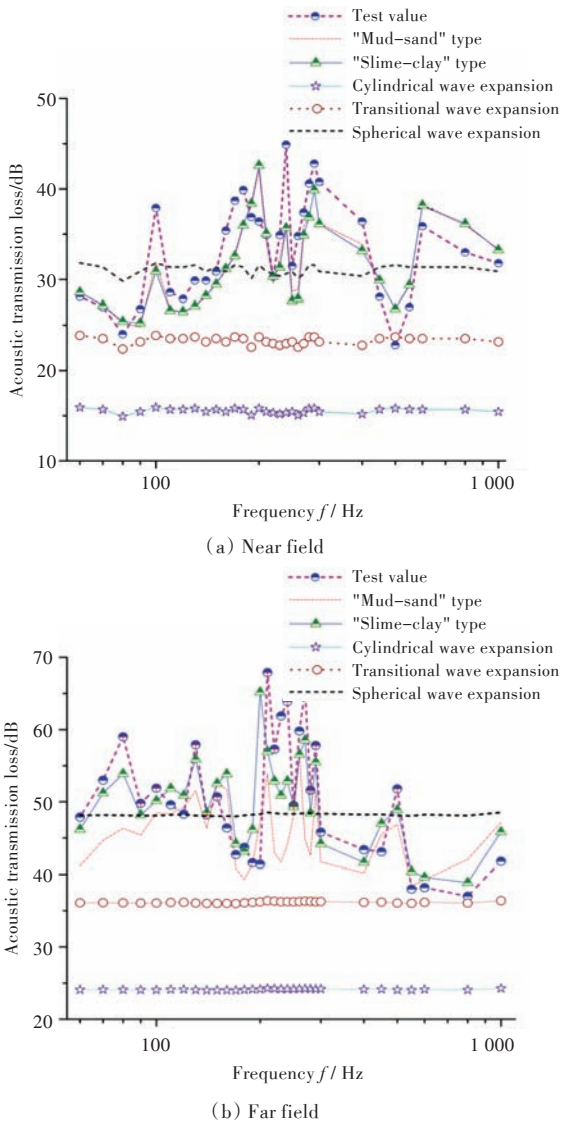

Fig.5 Simulation model comparison of transmission loss between the sedimentary layers

Fig. 5(a) showed that the near field transmission loss of "mud–sand" and "slime–clay" types of sedimentary layers model is almost the same, indicating the sedimentary layer type has small disturbance on the acoustic pressure distribution of near field points, which can be ignored. It can be seen from Fig. 5(b) that there is a large degree of separation between the 2 kinds of sedimentary layers models, in which the consistency between the "slime–clay" type of sedimentary layer model and the acoustic testing field is higher, hence the first choice for acoustic simulation.

3.1.2 Water level selection of simulation model

The testing field in limited water area is not a closed inland lake. Its water level would change with the rainy season, water storage period, etc., and the ideal test water level is about 70 m. From November of each year to January of the following year is the best test water level. In order to get the water level

that is more in line with the actual acoustic field, the acoustic transmission loss of water level H = 65, 70 and 75 m is simulated. Fig. 6 shows the comparison curves of acoustic transmission loss of different water levels in the near and far fields.

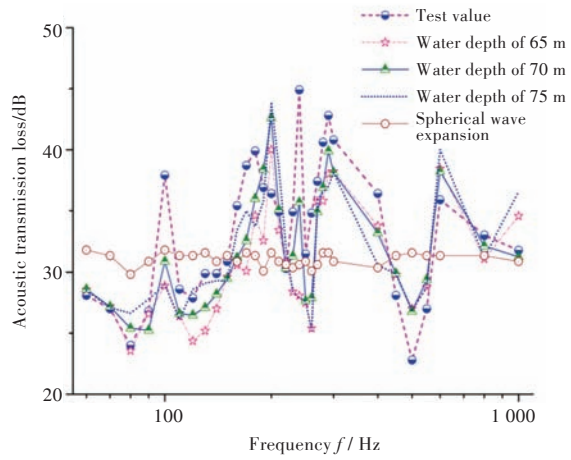

(a) Near field

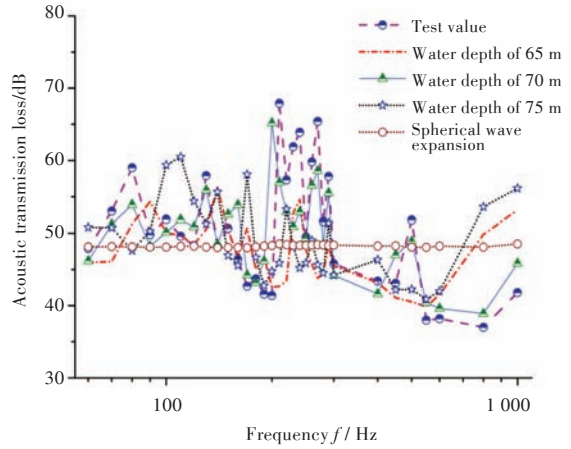

(b) Far field

Fig.6 Transmission loss curves comparison between different water levels

The comparison between simulation values and the test values of near field and far field transmission loss of 3 water levels shows that: when the water depth is 70 m, the simulation value is closer to the test value.

3.2 Simulation study of acoustic propagation characteristics

According to the comparison between the simulation values and test values of the "sedimentary layers" and water level, the "slime-clay" type of sedimentary layer model at water depth of 70 m is most in line with the actual acoustic field. In order to study the acoustic propagation characteristics of the testing field, this paper conducts simulating calculation on the impacts of non-dimensional parameter ξ of sound source with the fixed depth, source depth of fixed water depth and water surface roughness on the acoustic transmission loss, and gives the comparison curves of partial frequencies.

3.2.1 Influence of dimensionless parameter of sound source with fixed depth on the acoustic propagation characteristic of testing field

According to the acoustic shock excitation test, water depth of simulating sound source is fixed at 12.5 m. In order to study the effect law of surface and underwater on the acoustic transmission loss of testing field, the dimensionless parameter is defined as $\xi = \frac{H_s}{D}$, where H_s represents a fixed depth of sound source, and D is the distance from sound source to the underwater. The acoustic transmission loss is simulated and calculated in this paper when ξ = 1-5. Limited by the broadband property of simulating sampling, only the acoustic transmission loss contrast curves of 100, 200 and 400 Hz are given in this paper (Fig. 7).

We can see from Fig. 7 that, the impact of dimensionless parameter ξ on acoustic propagation characteristics of testing field is closely related to the horizontal distance and the frequency of sound source,

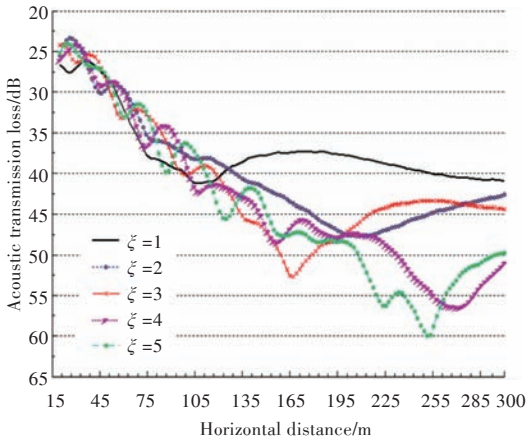

(a) f =100 Hz

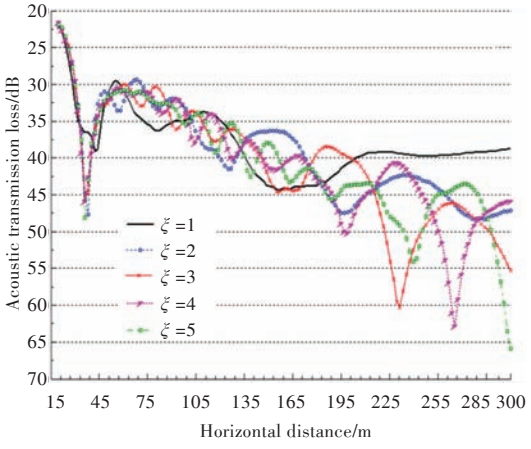

(b) f =200 Hz

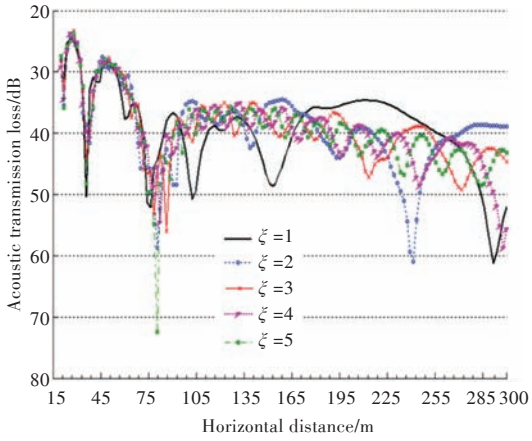

(c) f=400 Hz

Fig.7 Relationship between acoustic propagation characteristics and the dimensionless parameter of sound source

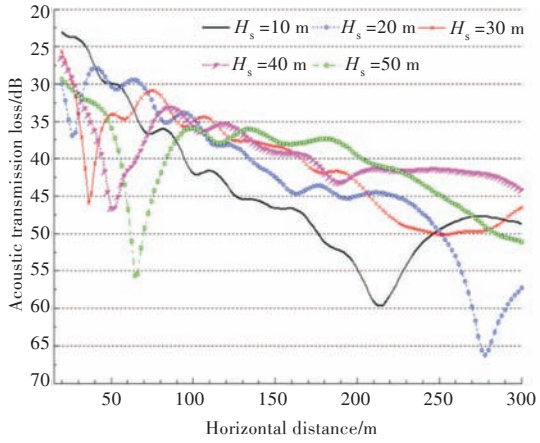

(a) f=100 Hz

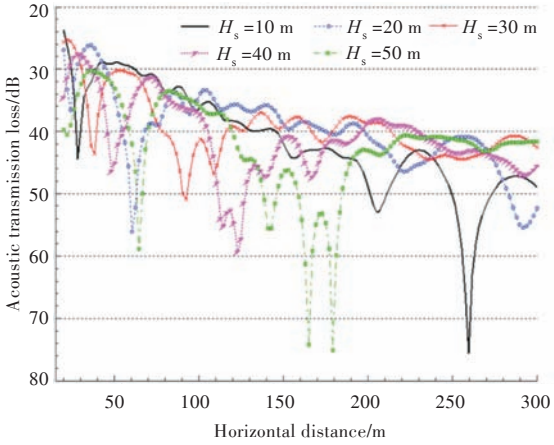

(b) f=200 Hz

Fig.8 Relationship between acoustic characteristics and the source depth

which generally presents the following characteristics:

1) The impact of dimensionless parameter ξ of the fixed-depth sound source on the acoustic propagation characteristics of testing field increases with the increasing horizontal distance.

2) The impact of ξ on the near field (within 60 m) acoustic transmission loss can be neglected. With the increase of the distance (especially more than 210 m), effect of ξ on the low frequency acoustic transmission loss is generally larger than that of the high frequency: at 100 Hz, the transmission loss difference between the models of ξ = 5 and ξ = 1 generally maintains at 10 dB; at 200 Hz, the difference maintains at 5–10 dB; at 400 Hz, the difference maintains at 5 dB. With the increase of frequency, the separation degree of transmission loss curve of ξ decreases obviously.

3.2.2 The influence of fixed-depth source position on the acoustic propagation characteristics of testing field

In order to explore the impact of source position on acoustic propagation characteristics of testing field, using the depth H_s of the sound source as independent variable, simulating calculation of the acoustic transmission loss is conducted when H_s = 10, 20, 30, 40 and 50 m, and the contrast curves of acoustic transmission loss at 100 and 200 Hz are presented (Fig. 8).

As can be seen from Fig. 8, the influence of source depth on acoustic transmission loss generally has the following characteristics:

1) At 100 Hz, the position of first trough on the transmission loss curve shifts backward with the increasing source depth, and the trough value increases accordingly; within 85 m, the transmission loss increases with the increase of the source depth; and in 85–220 m, the trend is opposite; in 220–300 m, acoustic transmission loss is the minimum at H_s= 40 m.

2) At 200 Hz, the acoustic transmission loss curves of various source depths are more complex, and the number of troughs increases significantly; within 190 m, acoustic transmission loss of each depth of the sound source alternates, and beyond 190 m, the closer the sound source is to the water surface, the greater the transmission loss is.

The simulating results show that the source position has a significant influence on the acoustic propagation characteristics of the testing field, and the effect law of the source depth on the acoustic transmission loss is closely related to the horizontal distance.

3.2.3 Influence of surface roughness on acoustic propagation characteristics of testing field

The test is in the daytime, and the solar radiation would lead to the "thermal convection", resulting in

waves on the surface of limited water area. This factor is defined as the RMS value of the surface roughness in the simulation program, and its physical meaning is the mean square wave height in Reference [5], whose relationship with the 1/3 effective wave height is:

$$H_{\text{rms}} = 0.704 H_{1/3} \tag{9}$$

$$H_{1/3} = 0.566 \times 10^{-2} V^2 \tag{10}$$

In the formula, V is wind velocity, kn. The calculated working conditions of wind velocity are shown in Table 2.

Table 2 Working conditions of calculation about roughness of water surface

Wind condition	Wind velocity V/kn	Mean square wave height H_{rms} /m
Breeze(level 3)	9	0.323
Moderate breeze(level 4)	15	0.897
Strong breeze(level 6)	25	2.500

To study the influence of surface roughness on acoustic transmission characteristics of testing field, this paper conducts simulating calculation on acoustic transmission loss in the wind conditions of breeze, moderate breeze and strong breeze, and gives the contrast curve of low frequency 150 Hz and high frequency 800 Hz (Fig. 9).

As can be seen from Fig. 9:

1) At a low frequency 150 Hz, the acoustic transmission loss curves of H_{rms} = 0.323 and 0.897 are basically consistent; except several points of peak and valley, the loss decreases with the increasing surface roughness when horizontal distance is within 33 m; in the range of 33–129 m, the trend is contrary; when it is more than 129 m, the loss value of the 3 roughnesses has alternately high and low trends, which is more obvious at the peak and valley.

2) At a high frequency 800 Hz, the degree of separation of the curves is larger than that of low frequency; on the whole, when the horizontal distance is within 37 m and in the range of 70–215 m, the loss decreases with increasing roughness; in the range of 37–70 m and beyond 215 m, the loss increases first and then decreases with the increase of roughness.

4 Incoherent analysis of deviation between experimental values and simulation values based on ray acoustics

The reason for incomplete consistence of experimental values and simulation values includes the

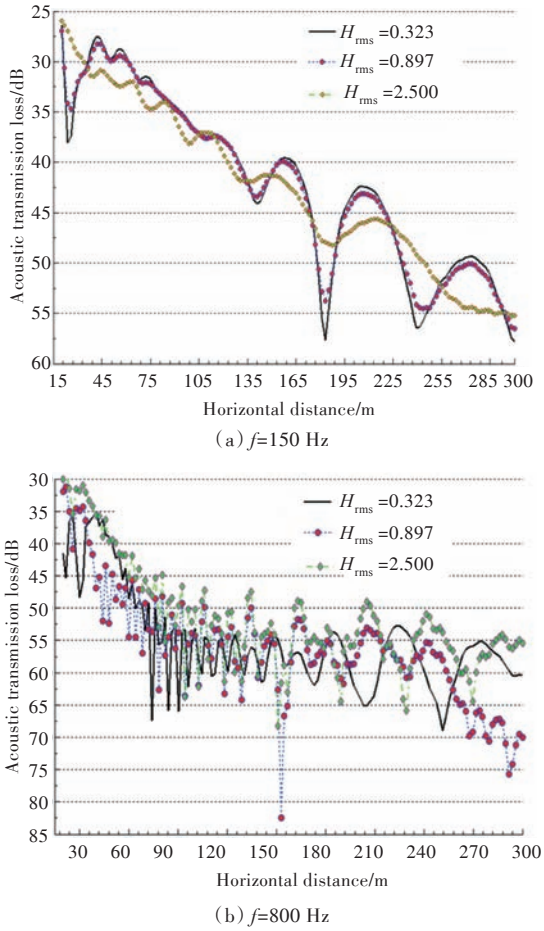

(a) f=150 Hz

(b) f=800 Hz

Fig.9 Relationship between acoustic characteristics and the roughness

geological features, boundary impedance conditions, electromagnetic interference, calculation accuracy, measurement error and boundary reflection, and surface and underwater reflection are the main influencing factors. In order to study the effect, based on ray acoustics, and ignoring the phase factors, only the acoustic pressure amplitude is considered to carry out incoherent analysis of deviation.

Eq. (2) is expanded. Let m = 0, and only the first 4 items of infinite formula are taken.

1) The expression of acoustic pressure in the free field is

$$P_{01} = \frac{1}{R_{01}} \mathrm{e}^{\mathrm{j}kR_{01}} = \frac{1}{R_{01}} \left(\cos kR_{01} + \mathrm{j} \sin kR_{01} \right) \tag{11}$$

2) When only one underwater reflection is considered, the acoustic pressure is

$$P_{02} = \frac{1}{R_{01}} \mathrm{e}^{\mathrm{j}kR_{01}} + \frac{1}{R_{02}} \mathrm{e}^{\mathrm{j}kR_{02}} = \left(\frac{1}{R_{01}} \cos kR_{01} + \frac{1}{R_{02}} \cos kR_{02} \right) + \mathrm{j} \left(\frac{1}{R_{01}} \sin kR_{01} + \frac{1}{R_{02}} \sin kR_{02} \right) \tag{12}$$

3) When only one surface reflection is considered, the acoustic pressure is

$$P_{03}=\frac{1}{R_{01}}\mathrm{e}^{\mathrm{j}kR_{01}}-\frac{1}{R_{03}}\mathrm{e}^{\mathrm{j}kR_{03}}=$$
$$\left(\frac{1}{R_{01}}\cos kR_{01}-\frac{1}{R_{03}}\cos kR_{03}\right)+$$
$$\mathrm{j}\left(\frac{1}{R_{01}}\sin kR_{01}-\frac{1}{R_{03}}\sin kR_{03}\right) \quad (13)$$

4) When only one surface reflection and one underwater reflection were considered, the expression of acoustic pressure was

$$P_{04}=\frac{1}{R_{01}}\mathrm{e}^{\mathrm{j}kR_{01}}+\frac{1}{R_{02}}\mathrm{e}^{\mathrm{j}kR_{02}}-\frac{1}{R_{03}}\mathrm{e}^{\mathrm{j}kR_{03}}-\frac{1}{R_{04}}\mathrm{e}^{\mathrm{j}kR_{04}}=$$
$$\left(\frac{1}{R_{01}}\cos kR_{01}+\frac{1}{R_{02}}\cos kR_{02}-\frac{1}{R_{03}}\cos kR_{03}-\right.$$
$$\left.\frac{1}{R_{04}}\cos kR_{04}\right)+\mathrm{j}\left(\frac{1}{R_{01}}\sin kR_{01}+\frac{1}{R_{02}}\sin kR_{02}-\right.$$
$$\left.\frac{1}{R_{03}}\sin kR_{03}-\frac{1}{R_{04}}\sin kR_{04}\right) \quad (14)$$

To study the influence characteristics of surface and underwater reflection on the near field and far field sound pressure levels, according to sound pressure expressions of Eq. (11)–(14) and Eq. (15), contrast curves of 4 theoretical models for the measurement of acoustic pressure level can be obtained (Fig. 10).

$$SPL=20\lg\left(P_{\mathrm{e}}/P_{\mathrm{ref}}\right) \quad (15)$$

where P_{e} is effective value of measured acoustic pressure; and P_{ref} is reference acoustic pressure, taken as 1×10^{-6} Pa in this paper.

Fig. 10 (a) shows that higher degree of agreement exists between the curves of dB–P_{01} and dB–P_{02}, and between dB–P_{03} and dB–P_{04}, which indicates that when the low frequency sound transmittes in the near field, the contribution value of underwater reflection on the testing field sound pressure level is small, and that of surface reflection wave is large, which is the main cause for the deviation.

Fig. 10 (b) shows that in the frequency range below 150 Hz, curves dB–P_{01} and dB–P_{02} are highly consistent, indicating that the surface reflection is the main cause of deviation when acoustic wave lower than 150 Hz transmits in the far field, while the influence of underwater reflection can be ignored; when higher than 150 Hz, curves dB–P_{01} and dB–P_{03} agreed well, indicating that when acoustic wave higher than 150 Hz transmits in the far field, the contribution value of underwater reflection on the testing field sound pressure level is greater than that of the water surface, but both affect the acoustic field distribution.

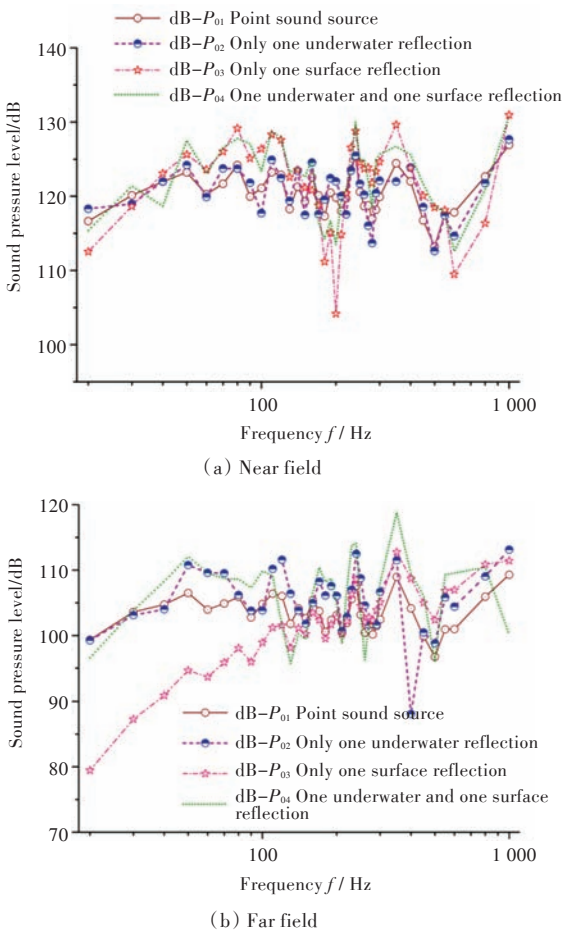

Fig.10 Comparison between four different theoretical models of sound pressure level at near and far field

5 Conclusions

In this paper, the acoustic propagation characteristics of testing field in limited water area are simulated by using AcTUP software, and the following conclusions are obtained by numerical and theoretical analysis:

1) The selection of "sedimentary layers" and water level affect the acoustic simulation effect of the testing field. The simulation model is closest to the actual working condition when the sedimentary layer is "slime–clay" type and the water depth is 70 m.

2) The influence of non-dimensional parameter ξ of fixed depth source, source depth and surface roughness on the acoustic propagation characteristic of testing field is closely related to frequency and horizontal distance.

3) When acoustic waves of low frequency and intermediate frequency (less than 1 000 Hz) transmit in the near field, contribution value of surface reflection wave is larger, which is the main cause for the deviation; in the far field, contribution value of underwater reflection on the testing field sound pres-

sure level is greater than that of the water surface, but both affect the acoustic field distribution.

References

[1] AI Haifeng, CHEN Zhijian, WANG Lu. Structural-acoustic analysis on the cabin of underwater vehicle[J]. Chinese Journal of Ship Research, 2010, 5(6): 12-15(in Chinese).

[2] LI Tianyun, WANG Lu, GUO Wenjie, et al. Vibration characteristics analysis of the finite cylindrical shells semi-filled with liquid[J]. Chinese Journal of Ship Research, 2016, 11(2): 106-110(in Chinese).

[3] JENSEN F B, KUPERMAN W A. Optimum frequency of propagation in shallow water environments[J]. The Journal of the Acoustic Society of America, 1983, 73(3): 813-819.

[4] JENSEN F B, KUPERMAN W A, PORTER M B, et al. Computational ocean acoustics[M]. New York: Spring, 1992.

[5] ETTER P C. Underwater acoustic modeling and simulation[M]. CAI Zhiming, Trans. Beijing: Electronic Industry Publishing House, 2005: 7(in Chinese).

[6] CHEN Peng. Study on sound propagation in shallow water environment[D]. Qingdao: Ocean University of China, 2014: 5(in Chinese).

[7] LIN Ju, ZHAO Yue, WANG Huan, et al. Analysis of deep sea acoustic propagation based on ray stability parameter[J]. Journal of Nanjing University (Natural Sciences), 2015, 51(6): 1223-1233(in Chinese).

[8] CHEN Fa, LI Yongsheng, ZHAO Gang, et al. Simulation of point target echo based on the actual hydrological conditions[J]. Torpedo Technology, 2015, 23(4): 311-315(in Chinese).

[9] CHEN Hongyang. Research on prediction of sound radiated by elastic structure in underwater bounded space[D]. Harbin: Harbin Engineering University, 2013(in Chinese).

[10] MAGGI A L, DUNCAN A J. AcTUP v2.2l$^{\alpha}$ (acoustic toolbox user-interface and post-processor) installation and user guide[R]. Australia: Centre for Marine Science and Technology, Curtin University of Technology.

[11] ZHANG Jun. FFP method based study of underwater low frequency sound propagation[D]. Changsha: National Defense Science and Technology University, 2008:11(in Chinese).

[12] LIU Bosheng, LEI Jiayu. 水声学原理[M]. Harbin: Harbin Engineering University Press, 1993: 92-94(in Chinese).

[13] URICK R J. Principles of underwater sound[M]. 3rd ed. New York: Peninsula Pub, 2006: 137-141.

有限水域试验场声传播特性的仿真计算与试验

仪修阳[1], 周其斗[1], 吴祥兴[2]

1 海军工程大学 舰船工程系,湖北 武汉 430033

2 杭州应用声学研究所, 浙江 杭州 310023

摘 要: 在有限水域试验场中进行大型复杂结构的水下声振试验,声信号测量和数据处理是关键。天然水域边界条件未知,水文环境复杂,仿真难度高,增加了数据处理难度。采用Matlab和VB混合编程软件AcTUP,分析试验场"沉积层和水位"的选取原则,得到与试验值较为吻合的仿真模型。通过仿真计算,得到固定深度声源的"无因次量纲"参数、固定水深的声源位置及水面粗糙度对试验场声传播损失的影响规律,并基于射线声学理论对试验值和仿真值的偏差进行非相干分析,得到了有限水域试验场的基本声传播特性。

关键词: 有限水域; 声学试验场; 声传播特性; 边界条件; AcTUP; 射线声学理论; 偏差